Extracellular and intracellular alkalinization and the constriction of rat cerebral arterioles

Michael Apkon*† and Walter F. Boron†

*Departments of *Pediatrics and †Cellular and Molecular Physiology, Yale University School of Medicine, New Haven, CT 06510, USA*

1. Direct observations of perfused cerebral arterioles *in vivo* and *in vitro* have demonstrated that alkalinization of blood or cerebrospinal fluid (CSF) causes arteriolar constriction. Inasmuch as such alkalinizations lead to increases in intracellular pH (pH_i) as well as interstitial pH (pH_o), it is possible that increases in either pH_i or pH_o (or both) underlie alkalinization-induced cerebral vasoconstriction. In order to test the hypothesis that changes in pH_i alone underlie allkalinization-induced cerebral vasoconstriction, we simultaneously measured vessel diameter and pH_i (using the pH-sensitive dye, SNAFL) in isolated cerebral arterioles from adult rats during imposed alterations in pH_o and pH_i.

2. Penetrating cerebral arterioles from the distribution of the middle cerebral artery were hand dissected, cannulated on one end and occluded distally. Vessels were inflated hydrostatically to 60 cmH_2O under no-flow conditions. Confocal microscopy verified specific pH-sensitive dye staining of the vascular smooth muscle cells within the vessel wall.

3. Extracellular alkalinization from pH 7·3 to 7·8 caused pH_i to increase by 0·06 ± 0·01 of a pH unit, and vessel diameter to decrease by 21·8 ± 1·8% (means ± S.E.M.).

4. Intracellular alkalinization at constant pH_o was produced by exposure to weak bases, including NH_3 and trimethylamine, or by exposure to, followed by withdrawal of, weak acids, including CO_2 and acetic acid. None of these treatments evoked vasoconstriction even though each of them caused increases in pH_i greater than those observed in the same vessels during exposure to the pH_o 7·8 solution.

5. We conclude that, at least in cerebral arterioles, alkalinization-induced vasoconstriction is mediated by an increase in pH_i, not pH_o.

H^+ and CO_2 have been postulated to play a major role in the regulation of cerebral vascular tone since Roy & Sherrington (1890) suggested that these metabolic end products might underlie the increase in cerebral blood flow that occurs with neural stimulation. Direct observation of perfused cerebral arterioles *in vivo* and *in vitro* have demonstrated that alkalinization of blood or cerebrospinal fluid (CSF) causes arteriolar constriction (Kontos, Raper & Patterson, 1977*a*; Kontos, Wei, Raper & Patterson, 1977*b*; Dacey & Duling, 1982). Inasmuch as such alkalinizations lead to increases in intracellular pH (pH_i) as well as interstitial pH (pH_o), it is possible that increases in either pH_i or pH_o (or both) underlie alkalinization-induced cerebral vasoconstriction. If pH_i were the sole determinant of the vasoconstriction, then it seems reasonable to suppose that the speed and extent of the vasoconstriction might depend critically on the ability of the buffer to penetrate the cell membranes of vascular smooth muscle and/or endothelial cells. For example, one might expect that respiratory alkalosis might, as a result of high membrane permeability to CO_2, produce a greater increase in pH_i and a more intense vasoconstriction than would metabolic alkalosis. However, because vasoconstriction may be elicited equally by respiratory or metabolic alkalosis in the interstitial fluid, several investigators have concluded that alkalinization-induced vasoconstriction is caused by increased pH_o rather than increased pH_i.

The validity of this interpretation depends on the relationship between changes in pH_i and pH_o during alkalosis. Although pH_i does indeed increase rapidly during respiratory alkalosis, this pH_i increase may only be transient; the subsequent pH_i trajectory may vary considerably, depending on the cell type. Furthermore, although the steady-state pH_i during extracellular respiratory alkalosis is likely to be greater than the initial

pH_i, the degree of intracellular alkalinization is unpredictable. Increases in pH_i caused by metabolic alkalosis also vary considerably, depending on cell type. In most cells, metabolic alkalosis causes a pH_i increase that is 20–30% as large as the pH_o increase (Ellis & Thomas, 1976; Tolkovsky & Richards, 1987; Wray, 1988). Mesenteric arteriolar smooth muscle and carotid body glomus cells, however, exhibit a $\Delta pH_i/\Delta pH_o$ greater than 80 (Austin & Wray, 1993) and 70%, respectively (Buckler, Vaughan-Jones, Peers, Lagadic-Gossman & Nye, 1991; Wilding, Cheng & Roos, 1992).

Increases in pH_i have been suggested to underlie alkalinization-induced constrictions in other vascular tissue. Mesenteric arterioles, which exhibit a large $\Delta pH_i/\Delta pH_o$, appear to constrict in response to increased pH_i rather than increased pH_o (Austin & Wray, 1993). Similarly, rat aorta appears to constrict upon intracellular alkalinization. Exposure to solutions containing NH_3/NH_4^+ causes a rapid intracellular alkalinization (at constant pH_o) of cultured rat aortic smooth muscle cells, and a slowly developing constriction of intact aortic rings (Danthuluri & Deth, 1989). These conclusions are in distinct contrast to the foregoing conclusion that alkalinization-induced constrictions in cerebral arterioles depend solely on increases in pH_o. Because alkalinization-induced constrictions are a general property of systemic arterioles, it would be surprising if the transduction mechanism for alkalinization-induced vasoconstriction in cerebral arterioles differed so remarkably from that of other systemic arterioles. This discrepancy may only be apparent, inasmuch as pH_i has not been measured in cerebral arteriolar smooth muscle. Thus, if respiratory and metabolic alkaloses cause similar increases in pH_i, then increases in pH_i alone may underlie alkalinization-induced constriction in cerebral as well as in other systemic arterioles.

In order to test the hypothesis that changes in pH_i alone underlie alkalinization-induced cerebral vasoconstriction, we simultaneously measured pH_i and vessel diameter in isolated, cannulated penetrating cerebral arterioles from adult rats during imposed alterations in extralumenal pH_o and/or pH_i. We found that increases in pH_o, but not increases in pH_i, caused cerebral vasoconstriction. Preliminary accounts of this work have been published in abstract form (Apkon & Boron, 1994*a*, *b*).

METHODS

Preparation of penetrating cerebral arterioles

Penetrating cerebral arterioles in the distribution of the middle cerebral artery (MCA) were prepared from adult male rats according to the protocol of Dacey & Duling (1982). Briefly, adult male rats (250–300 g) were anaesthetized with methoxyflurane and decapitated. The skull was opened, the dura mater was stripped away and the brain was transferred *en bloc* to an ice-cold physiological saline solution (PSS) and then to the refrigerated stage (4 °C) of a dissecting microscope. A square region of neocortex, 1 cm^2 and approximately 5 mm thick, representing the distribution of the MCA, was excised. The pial membrane was elevated and retracted gently, preserving the penetrating arterioles arising from the primary branches of the MCA. The adventitial surfaces of penetrating arterioles were cleaned by dissection with sharpened forceps, although vessels isolated in this manner were largely free of attached connective tissue. An unbranching segment of arteriole (35–60 μm diameter, 0·5–2 mm long) was then removed by transection with sharpened iridectomy scissors and transferred, using a fire-polished glass pipette, to a chamber on the stage of an inverted microscope (IM35, Zeiss Inc., Thornwood, NJ, USA).

Cannulation and inflation of vessels

One end of the arteriole was drawn into the mouth of a glass holding pipette fabricated to have an hourglass-shaped constriction near the end. The vessel was then cannulated with a glass micropipette ('perfusion pipette'; 15 μm tip diameter) mounted on a motorized holder (Luigs and Neuman, Frankfurt, Germany) and held concentrically within the holding pipette. The vessel was sealed by compressing it between the perfusion pipette and the constriction in the holding pipette. This approach was originally used to perfuse renal tubules (Burg, Grantham, Abramow & Orloff, 1966) and was adapted by others to perfuse arterioles (Duling, Gore, Dacey & Damon, 1981). The perfusion pipette was attached to a reservoir of PSS at a height 60 cm above the microscope stage. With initiation of perfusion, the vessel lumens cleared of red blood cells within 1–2 s and the vessels distended slightly. The opposite end of the vessels was then approached with a second glass holding pipette and sealed shut by drawing the side of the vessel into the pipette to create a hairpin loop. The holding pipettes were manipulated so that the vessel segments were straight but not stretched, and so that a horizontal longitudinal plane through the centre of the vessel lumen intersected a single plane of focus. Continuity of the perfusion pipette and the vessel lumen was verified in all experiments by observing prompt collapse of the vessels when the perfusion pipette housing was vented to atmosphere. The absence of leaks was verified by observing a constant vessel diameter for at least 30 s after the connection between perfusion pipette and reservoir was occluded. Under these conditions, there was *no flow* through the vessel and the intralumenal pressure was constant at 60 cmH_2O. A pressure of 60 cmH_2O was chosen as this pressure is great enough to induce spontaneous tone (myogenic response) in these vessels and results in vessel diameters in the mid-range of the pressure–diameter relationship (Dacey & Duling, 1982, 1984). As there was no flow through the vessel the lumenal solution remained constant during all experiments. The external surface of the vessels (the 'bath') was superfused with solutions heated to 37 °C.

Microscopy

Cannulated arterioles were viewed through an inverted microscope mounted upon a vibration isolation table (Newport Corp., Fountain Valley, CA, USA). The plane of focus was set and maintained at the level where the apparent lumen diameter was widest and the lumenal margins the sharpest. Light paths for trans-illumination and epi-illumination are illustrated in Fig. 1. The specimen was trans-illuminated with light from a halogen lamp through a computer-controlled shutter and a 600 nm long-pass optical filter. Filtering this trans-illuminating light minimized photobleaching of the fluorescent dyes used to measure intracellular pH. Additionally, the preparation was epi-

illuminated with light at two wavelengths generated by a second halogen lamp, through a system of computer controlled shutters, filters and dichroic mirrors (see Boyarsky, Ganz, Sterzel & Boron, 1988). The transmitted and fluorescent images were collected by a ×20 objective and passed through the microscope to an image splitter (Multiimage Module, Nikon Co., Tokyo); 90% of the light was transmitted to a photomultiplier tube (PMT; model R1104, Hamamatsu Photonics, Hamamatsu City, Japan) used to measure the intensity of the fluorescence images, and 10% of the light was transmitted to a video camera (model NC-67MD, Dage-MTI Co., Michigan City, IN, USA) to detect transmitted images for measuring vessel diameter. A variable gain, computer-controlled integrating amplifier (typically integrating the signal at each excitation wavelength for 200 ms) magnified the PMT current for sampling by an analog-to-digital converter (Boyarsky *et al.* 1988). Transmitted images detected by the video camera were digitized using a video processor (model AFG, Imaging Technologies Inc., Woburn, MA, USA) and stored on hard disk. Program macros written for OPTIMAS (Optimas Co., Edmonds, WA, USA) on an Intel 80486 processor-based personal computer controlled the timing of all shutters, sampling of video images, and the measurement of fluorescence intensity by the PMT. Each complete sample cycle consisted of measuring the intensities of fluorescence excited by epi-illumination at each of two wavelengths, as well as acquiring one transmitted image. This sample cycle was repeated at intervals of 10–30 s.

Intralumenal vessel diameters were measured 'off-line' from these images by calculating the distance between the lumenal margins along a line perpendicular to the lumen axis. Lumenal margins were detected automatically according to an intensity profile matching algorithm within OPTIMAS; each image was examined at analysis time to verify proper detection of the lumen margin.

Measurement of intracellular pH

Intracellular pH was measured with the pH-sensitive fluorophores 2,7-biscarboxyethyl-5(6)-carboxyfluorescein (BCECF) or 5′,6′-carboxy-3,10-dihydroxy-spiro[7H-benzo[c]xanthene-7,1′(3′H)-isobenzofuran]-3′-one (SNAFL) using a dual-excitation, single-emission ratiometric technique (Boyarsky *et al.* 1988). Cells within cannulated arterioles were loaded with dye by exposing the cells to PSS containing 10 μM of the membrane-permeable form of the dye (AM form of BCECF; diacetate form of SNAFL) from the bath. Vessels were allowed to load dye for 30 min at 37 °C, and were then rinsed with PSS. BCECF was excited alternately at 440 and 490 nm, and light emitted at 530 ± 5 nm (I_{440} and I_{490}) was measured. pH_i was calculated from the ratio I_{490}/I_{440} using a variation of the high-$[K^+]$ Nigericin technique (Thomas, Buchsbaum, Zimniak & Racker, 1979). We used a single-point calibration procedure, terminating each experiment by determining the I_{490}/I_{440} ratio at a pH_i of 7·00 and then normalizing all data in that experiment to the ratio at pH_i 7·00 (Boyarsky *et al.* 1988). A detailed calibration curve, relating the I_{490}/I_{440} ratio to pH over a range of pH_i values, was obtained on three vessels. The pK value was 7·46 ± 0·06, and the scaling factor was 1·54 ± 0·05.

When pH_i was measured using SNAFL, the excitation wavelengths were 515 ± 5 and 535 ± 5 nm, and the emission

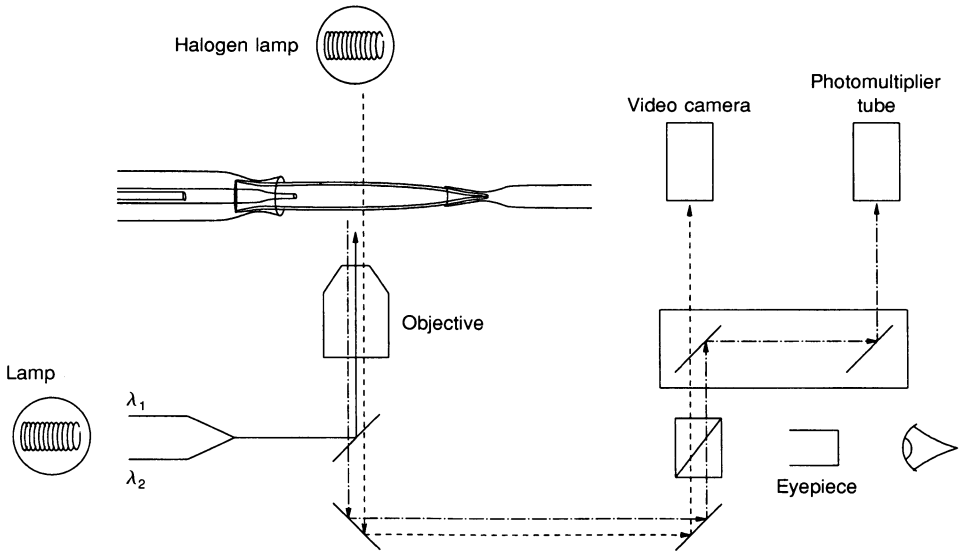

Figure 1. Schematic diagram of the light-path for simultaneous measurement of intracellular pH and vessel diameter

An isolated arteriole is shown mounted on the stage of an inverted microscope. One end of the vessel was cannulated to allow inflation, and the opposite end of the vessel was occluded to establish no-flow conditions. The specimen was trans-illuminated with light from a halogen bulb and epi-illuminated by light at two alternating wavelengths (λ_1 and λ_2). Computer-controlled shutters determined the illumination source. Light passing through the specimen, or fluorescent light originating from the specimen, was collected by the objective and transmitted through the microscope to an image splitter. The image splitter directed 90% of the light to a photomultiplier tube for quantitation of the fluorescent intensity and the remaining 10% of the light to a video camera for detection of the trans-illuminated image. The video images were digitized and stored on computer disk for later determination of vessel diameter.

wavelength was 605 ± 27·5 nm. SNAFL was calibrated using a method similar to that described for BCECF. The pK value was 7·02 ± 0·04, and the scaling factor was −1·69 ± 0·07 ($n = 7$; Boyarsky *et al.* 1988).

In both the BCECF and SNAFL experiments, fluorescent light was collected from an area ~200 μm in diameter in the specimen plane. The pH_i measured was thus a volume-weighted average of the pH_i of cells within this field. Vascular tissue is composed of connective tissue and cellular elements, including endothelial cells, vascular smooth muscle cells and fibroblasts. The contribution of fluorescence emission from each of these cell types depends on the relative frequency, volume and pH_i value of each cell, as well as the relative intracellular dye concentration. The contribution of fluorescence from endothelial cells was expected to be small for several reasons. (1) The total cell volume of the endothelial cells can be expected to be small relative to that of the vascular smooth muscle cells. (2) The dye was loaded from the bath side of the vessel rather than from the lumen, which contains dye-free solution. (3) We made no attempt to preserve endothelial integrity, such as by including protein in the lumenal solution; it has been reported that such measures are essential for preserving the endothelium (Duling *et al.* 1981). The contribution of fluorescence from fibroblasts was also expected to be minimal, inasmuch as they are present in greatest numbers within the vessel adventitia, which is greatly attenuated in penetrating cerebral arterioles (Pease, 1962). Indeed, the vast majority of the cell mass within the cerebral arterioles is contained within the media, composed almost exclusively of smooth muscle cells and extracellular matrix (Rhodin, 1980).

To verify that fluorescent light arose primarily from smooth muscle cells, several isolated but uncannulated arterioles were loaded with BCECF on the stage of a confocal microscope (Laserscan, Zeiss Inc.). After dye loading, fluorescence was easily observable within a single layer of spindle-shaped cells arranged circumferentially around the vessel which are presumed to be vascular smooth muscle cells (Fig. 2). At higher gain levels, irregular staining of the lumenal margin was observed, which is consistent with dye uptake (albeit to a much lesser degree) by endothelial cells. No other dye uptake was observed. Thus it appears that the vast majority of the fluorescence arises from smooth muscle cells.

During initial experiments, which were performed with BCECF, we frequently noted an irreversible vasoconstriction that was limited to the epi-illuminated segment of the perfused arteriole.

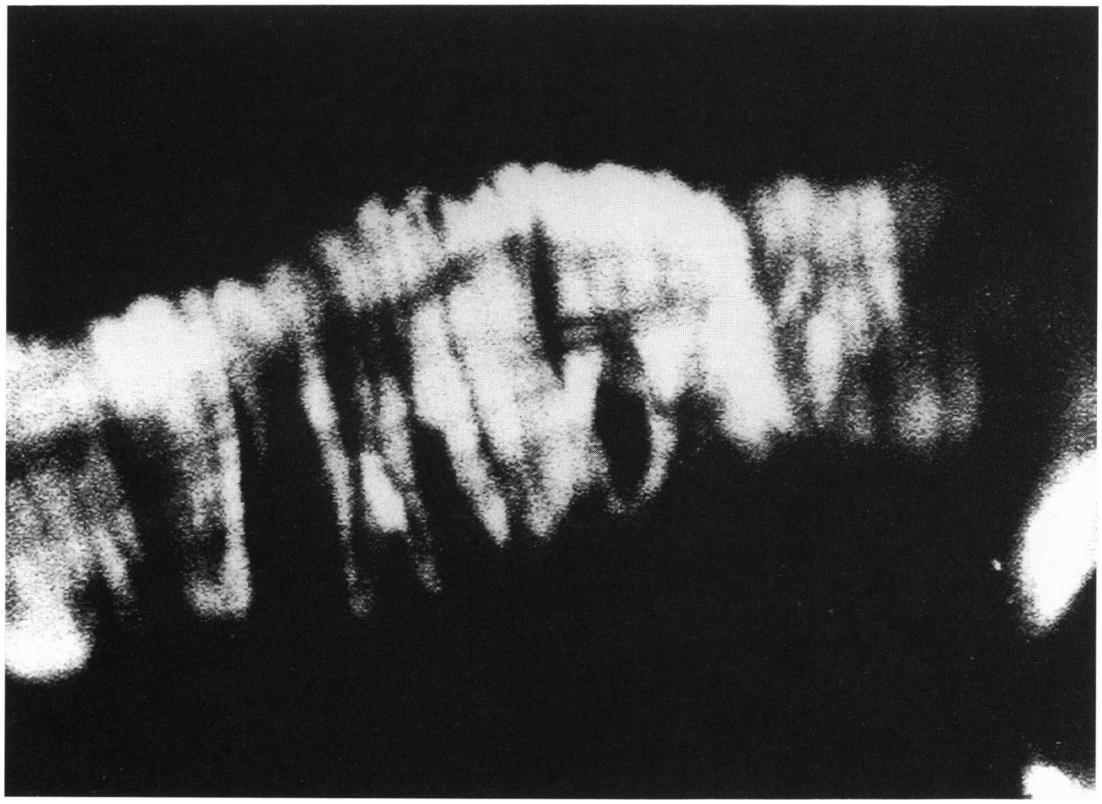

Figure 2. Confocal image of a penetrating cerebral arteriole after exposure to BCECF

The vessel was bathed in a solution containing 10 μM BCECF. Dye uptake is demonstrated in circumferentially oriented spindle-shaped cells consistent with staining of vascular smooth muscle cells. Microscopy was performed using a laser scanning confocal microscope equipped with a ×50, 1·2 numerical aperture lens (E. Leitz Inc, Rockleigh, NJ, USA). The pinhole used in these experiments provided a theoretical sampled thickness of 0·1 μm. Excitation illumination in this experiment was provided by a 50 mW krypton–argon laser. The excitation wavelength was 488 nm and the emitted light passed through a long-pass filter with a 515 nm cut-off. The diameter of this arteriole is approximately 60 μm.

The onset of this vasoconstriction was earlier and the magnitude greater when the dye concentration was greater, the excitation illumination more intense or the superfusing solution equilibrated with a 95% O_2–5% CO_2 mixture rather than air. At lower illumination intensities, this vasoconstriction was not observed. In several experiments, however, the vasomotor response to various experimental manipulations was lost in the epi-illuminated area, but preserved along the remainder of the vessel segment. These phenomena were not observed when pH_i was measured with SNAFL, except occasionally when solutions were equilibrated with a 95% O_2–5% CO_2 mixture. Because the irreversible vasoconstriction and loss of vasomotion were observed only within the epi-illuminated field, and because both were accentuated by increases in dye concentration and illumination intensity, these effects probably reflect dye-dependent, photodynamic damage. In order to minimize photodynamic damage, all further experiments were done using SNAFL to measure pH_i. The illumination intensity was set to as low a value as possible, consistent with a reasonable signal-to-noise ratio. All solutions were equilibrated with room air unless otherwise specified.

Solutions

The pH of all solutions was measured, gas equilibrated, and titrated at 37 °C using an Orion pH meter (Model 811, Orion Research Inc., Cambridge, MA, USA). The lumenal solution and initial bathing solution in all experiments was a Hepes-buffered physiological saline solution with the following composition (mM): NaCl, 125; KCl, 3; $MgSO_4$, 1·2; $CaCl_2$, 1; NaH_2PO_4, 2; glucose, 10·5; and Hepes, 32. This solution was titrated to pH 7·3 (at 37 °C) using NaOH (~18 mM) and equilibrated with room air. Solutions containing sodium acetate, NH_4Cl or trimethylamine chloride were identical, except that these substances replaced NaCl isotonically. Experiments were also performed in HCO_3^--buffered solutions. The standard HCO_3^--buffered solution was identical to the above solution except that Hepes was omitted and the solution contained 133·4 mM NaCl and 17 mM $NaHCO_3$. This solution had a pH of 7·3 when equilibrated with 5% CO_2 in air (at 37 °C). Respiratory alkalosis was produced by equilibration of this solution with 2·5% CO_2 in air (pH 7·6). Isohydric hypocapnia (pH 7·3) was produced by reducing the $NaHCO_3$ to 8·5 mM in exchange for NaCl and equilibrating with 2·5% CO_2. Each experiment was concluded by perfusion of the chamber with a high-K^+ solution containing (mM): KCl, 105; *N*-methyl-D-glucamine chloride, 43·8; $MgSO_4$, 1·2; $CaCl_2$, 1; H_3PO_4, 2; glucose, 10·5; Hepes, 32; and nigericin, 0·01. This nigericin solution was titrated to pH 7·0 using HCl.

Statistics

All results are expressed as means ± S.E.M. Student's paired *t* test was used for statistical comparisons. $P < 0.05$ was considered to be statistically significant.

RESULTS

Initial values

The initial pH_i of vascular smooth muscle cells (VSMCs) within cannulated penetrating cerebral arterioles was 7·43 ± 0·01 in Hepes-buffered PSS at pH_o 7·3 ($n = 38$). The initial resting diameter of these vessels was 62·5 ± 2·2 μm. Although we sometimes observed significant low-frequency contractions randomly during experiments, vessels spontaneously returned to their initial diameter. In bicarbonate-buffered PSS at pH_o 7·3, the steady-state pH_i was 7·43 ± 0·02 and the diameter was 63·8 ± 3·3 μm ($n = 18$). For these eighteen cells, the application of CO_2–HCO_3^- caused a mean pH_i change of 0·00 ± 0·09 (not significant).

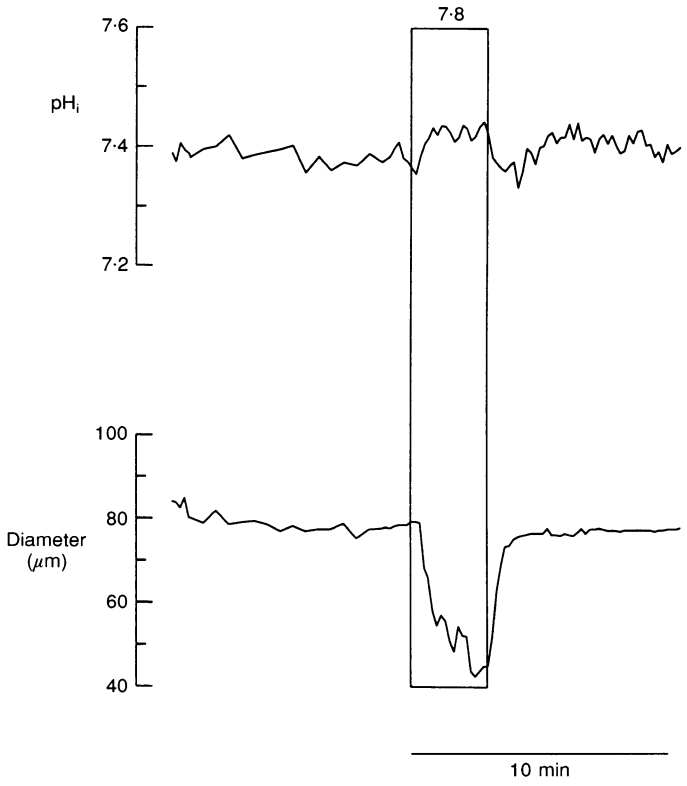

Figure 3. Recording of pH_i and intralumenal diameter during extracellular alkalinization from pH 7·3 to 7·8

After an equilibration period of bath perfusion with Hepes-buffered physiological saline at pH 7·3, the vessel was bathed with an identical solution titrated to pH 7·8 (□). Extracellular alkalinization to pH 7·8 resulted in a small increase in pH_i and a rapidly developing, reversible vasoconstriction.

Elevation of pH_o increases pH_i and causes vasoconstriction

We found that the pH_i of cerebral arterioles increases and vessel diameter decreases when pH_o was increased. As shown in Fig. 3, superfusing a vessel with Hepes-buffered PSS titrated to pH 7·8, rather than 7·3, caused a small increase in pH_i and a rapid, reversible constriction. In thirty-eight vessels, the mean increase in pH_i was $0·06 \pm 0·01$ of a pH unit, and the mean decrease in diameter was $21·8 \pm 1·8\%$ of the initial diameter. Contraction was graded at pH_o values less than 7·8 (not shown); elevating pH_o above 8·0 caused irreversible contraction and loss of dye from the preparation.

We also observed an increase in pH_i and decrease in diameter when we increased pH_o in CO_2–HCO_3^--buffered solutions. Figure 4 shows an experiment in which we first examined the effect of increasing the pH of a Hepes-buffered PSS from 7·3 to 7·8, and then exposed the vessel to our standard CO_2–HCO_3^--buffered saline. When the pH_o of the bath solution was then increased from 7·3 to 7·6 by halving the P_{CO_2} at a constant $[HCO_3^-]$ of 17 mM (a respiratory alkalosis), pH_i rapidly and monotonically increased by an average of $0·15 \pm 0·01$ ($n = 7$). Although this is more than twice the alkalinization observed in Hepes-buffered solutions, the decrease in vessel diameter was only $6·7 \pm 2·1\%$ ($n = 7$), approximately one-third the change observed in Hepes-buffered solutions. Thus, a comparison of the data obtained in Hepes- and CO_2–HCO_3^--buffered solutions suggests that an increase in pH_o may be more important in causing vasoconstriction than an increase in pH_i.

Elevation of pH_i at constant pH_o does not cause vasoconstriction

In order to raise pH_i at constant pH_o, we exposed vessels to PSS solutions in which we isotonically replaced some of the Na^+ with the protonated conjugate weak acid (e.g. NH_4^+) of a neutral weak base (NH_3) (Boron & De Weer, 1976). Exposing an arteriole to a solution containing 20 mM NH_3–NH_4^+ at a constant pH_o of 7·3 caused a large and rapid increase in pH_i (Fig. 5*A*) as the unprotonated, electroneutral form penetrated the cell membrane and combined with H^+, establishing an intracellular equilibrium between NH_3 and NH_4^+. This alkalinization was followed by a slower decline over a 2–4 min plateau phase, reflecting various acid loading processes, including the slower entry of the protonated weak acid, NH_4^+. The mean increase in pH_i, averaged over the time of the plateau phase of the NH_3–NH_4^+ exposures, was $0·29 \pm 0·04$ units ($n = 11$; Table 1). In approximately a quarter of the vessels, the initial exposure to NH_3–NH_4^+ was accompanied by a rapid, transient constriction (not shown). These constrictions never lasted longer than 10 s (our typical sampling interval) and completely reversed, despite continued presence of the NH_3–NH_4^+. Often, the constriction, although visible by eye, was too short-lived to be recorded by our imaging system. We suspect that these transient constrictions reflect small membrane depolarizations caused by the NH_4^+, which can permeate the cell membrane in other cell types (Binstock & Lecar, 1969; Hille, 1973). In no experiment did we observe a sustained decrease in vessel diameter, despite pH_i increases that were consistently greater than those elicited by raising pH_o to 7·8.

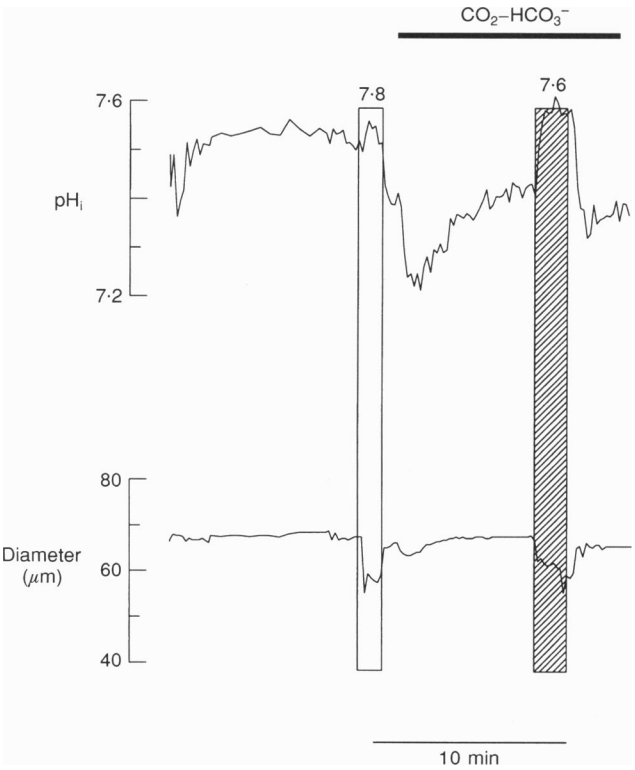

Figure 4. Recording of pH_i and intralumenal diameter during extracellular alkalinization in CO_2–HCO_3^--buffered solutions

After equilibration in Hepes-buffered PSS (pH 7·3), vascular reactivity was examined by exposure to the pH 7·8 PSS solution (□). At the time indicated, the bath solution was switched to a CO_2–HCO_3^--buffered solution (5% CO_2–17 mM HCO_3^-) at the same pH (i.e. 7·3). On introduction of the CO_2–HCO_3^- solution, pH_i fell transiently and a small transient vasoconstriction was observed. After stabilization of pH_i, the bath solution was changed to an identical CO_2–HCO_3^- solution, except that it was equilibrated with 2·5% rather than 5% CO_2; thus, pH_o increased to 7·6 (▨). A rapid increase in pH_i was observed as well as a decrease in diameter. Both the increase in pH_i and the decrease in diameter reversed upon return to the pH 7·3 (5% CO_2) solution.

The washout of NH_3–NH_4^+ from the bath in the experiment shown in Fig. 5*A* caused a rapid decrease in pH_i, followed by a slower pH_i recovery to the initial value. The rapid acidification evoked by NH_3–NH_4^+ washout is due to the efflux of the weak base, NH_3, whereas the pH_i recovery appears to be due to Na^+–H^+ exchange (Apkon & Boron, 1993). In some experiments (see 10 and 20 mM NH_4^+ pulses in Fig. 5*B*, below), the rapid acidification was accompanied by a constriction that developed quickly but decayed slowly. The time course of this decay paralleled the time course of pH_i recovery. That the vessel was capable of constricting in response to extracellular alkalinization in this experiment is shown by the response to an increase in pH_o from 7·3 to 7·8.

In order to reduce the likelihood of any potentially toxic effect of NH_3–NH_4^+, we repeated the experiments at NH_3–NH_4^+ concentrations of 5 and 10 mM, as well as 20 mM (see Fig. 5*B*). None of these NH_3–NH_4^+ solutions caused vasoconstriction, even though they all caused pH_i increases that were greater than those caused by paired treatments with a pH 7·8 Hepes-buffered solution.

To rule out further the possibility that NH_3–NH_4^+ toxicity prevented an intracellular alkalinization-induced constriction, we examined the effects of a second weak base on pH_i and vasoconstriction. As shown in Fig. 5*C*, we found that exposing a vessel to 20 mM trimethylamine–trimethylammonium (TMA) caused changes in pH_i similar to those produced by NH_3–NH_4^+ (Table 1). The effects of TMA on vessel diameter were also similar to those seen with NH_3–NH_4^+. In particular, we occasionally saw brief (<10 s) constrictions upon introducing TMA to the bath, but no sustained decreases in vessel diameter. Moreover, in about half of our experiments, washout of TMA led to rapidly developing, slowly decaying constrictions.

A third approach for minimizing the possible toxic effects of NH_3–NH_4^+ is to produce the intracellular alkalinization not by exposing cells to a weak base, but by withdrawing a weak acid. An example is shown in Fig. 6*A*, an experiment in which we briefly exposed a vessel to a solution containing 20 mM sodium acetate. The application of acetate caused a rapid pH_i decrease, due to the influx of acetic acid, followed during the plateau phase by a partial recovery, presumably due to Na^+–H^+ exchange as well as other acid-extrusion processes. In five experiments, the mean pH_i decrease, measured at the nadir of the plateau phase, was 0·29 ± 0·04. The initial acetate-induced acidification was frequently accompanied by a transient constriction, the relaxation of which was complete by the time pH_i stabilized. The subsequent withdrawal of the acetate produced a rapid alkalinization, due to the efflux of acetic acid, that reached a value greater than the initial pH_i. The mean pH_i overshoot in five such experiments was 0·08 (Table 1). However, we observed no decrease in vessel diameter in these experiments, even though the alkalinizations on acetate

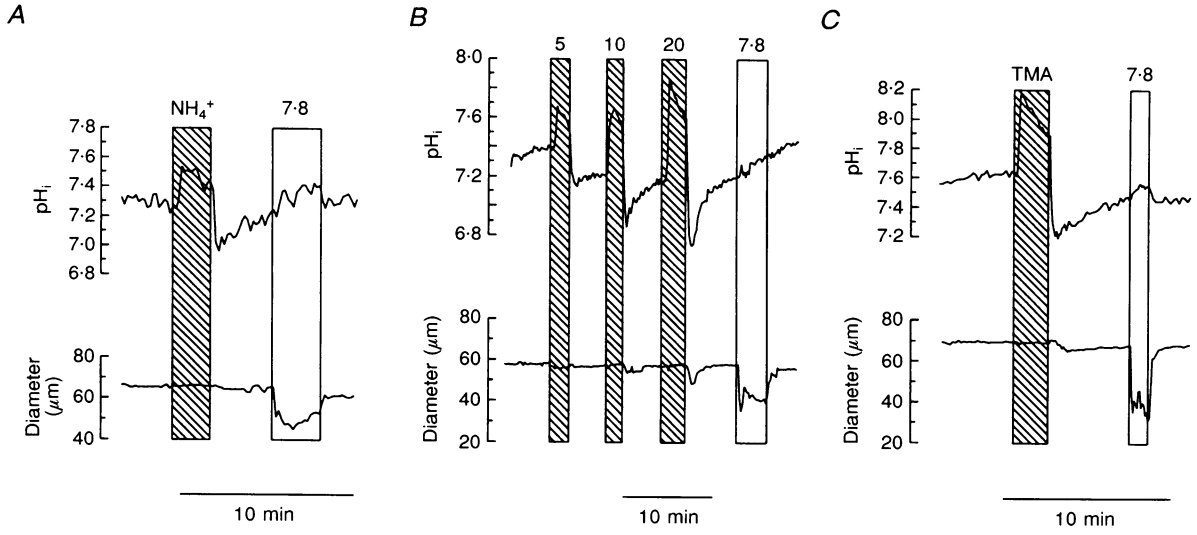

Figure 5. Recording of pH_i and intralumenal diameter during intracellular alkalinization by exposure to weak bases

A and *C*, intracellular alkalinization at constant pH_o was produced by exposure to bath solution containing 20 mM NH_4Cl (*A*) or trimethylamine chloride (TMA; *C*) which replaced NaCl isotonically. No vasoconstriction was observed during NH_4Cl or TMA exposures (▨) although extracellular alkalinization to pH 7·8 in a Hepes-buffered solution produced the usual alkalinization-induced vasoconstriction (□). *B*, similar experiment to *A* except that NH_4Cl was applied at three different concentrations (5, 10 and 20 mM; ▨). Vasoconstriction was not observed at any of the NH_4Cl concentrations despite increases in pH_i greater than that observed with extracellular alkalinization to pH 7·8 (□), an effective vasoconstrictor in this vessel.

Table 1. Comparison of effects on pH_i and vessel diameter of alkalinization by weak base exposure or weak acid washout (the 'treatment') with effects of alkalinization by exposure to high pH_o solutions

		pH_i			Diameter		
			Change (pH units)			Change (%)	
Treatment	n	Initial	Treatment	pH_o 7·8	Initial (μm)	Treatment	pH_o 7·8
NH_4^+ (20 mM)	11	7·41 ± 0·02	0·29 ± 0·04	0·10 ± 0·02*	64·2 ± 3·9	−0·3 ± 0·5	−19·8 ± 3·0*
TMA (20 mM)	4	7·49 ± 0·07	0·37 ± 0·04	0·03 ± 0·02*	53·8 ± 6·3	−0·5 ± 0·3	−25·8 ± 6·0*
Acetate washout (20 mM)	5	7·45 ± 0·05	0·08 ± 0·01	0·04 ± 0·01*	60·4 ± 5·9	−3·3 ± 1·4	−25·3 ± 6·0*
CO_2 washout (5%)	18	7·43 ± 0·00	0·11 ± 0·00	0·04 ± 0·00*	63·9 ± 3·3	0·9 ± 0·8	−21·2 ± 2·8*

The first column contains the 'treatment' compared (in each vessel) with extracellular alkalinization to pH 7·8 and concentration of base or acid applied; the second column shows the number of vessels studied. The means ± S.E.M. of the initial value for pH_i (prior to exposure to the treatment or high pH_o solutions) and the changes in pH_i produced by the treatment and pH_o 7·8 solution are reported for each treatment. Similarly, means ± S.E.M. of the initial value for vessel diameter (μm) (prior to exposure to treatment or high pH_o solutions) and the percentage changes in diameter produced by the treatment and pH_o 7·8 solution are reported. The changes in pH_i and diameters produced by the treatment and pH_o 7·8 were compared by Student's two tailed t test; * Statistically significant ($P < 0·05$) differences between the effects of the treatment and pH_o 7·8.

withdrawal were greater in paired experiments than the pH_i increases elicited by raising pH_o to 7·8 (Table 1).

Application and then withdrawal of CO_2–HCO_3^- produced changes in pH_i similar to those evoked by acetate exposure (Fig. 6*B*). The withdrawal of CO_2–HCO_3^- produced a pH_i increase of 0·11 without a change in vessel diameter (Table 1). A variation on this approach is to raise pH_i at constant pH_o by reducing $[CO_2]$, but not all the way to zero (i.e. a more modest isohydric hypocapnia). In seven experiments, we found that switching from a bathing fluid containing 5% CO_2–17 mM HCO_3^- at

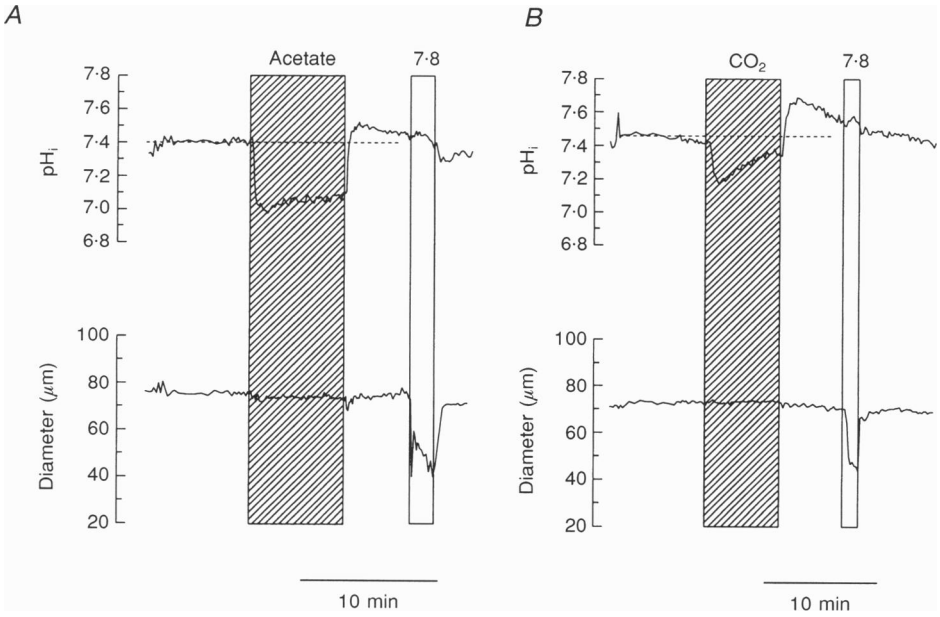

Figure 6. Recording of pH_i and intralumenal diameter during intracellular alkalinization by withdrawal of weak acids

Exposure to acetic acid (*A*) or to CO_2 (*B*) caused a decrease in pH_i followed by a slower partial recovery (▨). Withdrawal of these weak acids caused a rapid increase in pH_i to values greater than the initial resting pH (illustrated by the dashed lines). No vasoconstriction was observed despite increases in pH_i to values greater than that produced by extracellular alkalinization to pH 7·8, which was an effective vasoconstrictor in these vessels (□). In *A*, 20 mM sodium acetate replaced an equivalent amount of NaCl in the Hepes-buffered PSS. In *B*, the Hepes-buffered PSS was replaced with a CO_2–HCO_3^--buffered solution (5% CO_2–17 mM HCO_3^-).

pH 7·3 to one at the same pH but buffered with 2·5% CO_2–8·5 mM HCO_3^- caused pH_i to increase by 0·13 ± 0·01 with no decrease in diameter.

DISCUSSION

The experiments presented here demonstrate that increases in pH_o exclusively underlie alkalinization-induced cerebral vasoconstriction in adult rats. By simultaneously measuring pH_i and vessel diameter in isolated cannulated penetrating cerebral arterioles, we have shown that increases in pH_o cause vasoconstriction even though they lead to only small increases in pH_i. On the other hand, even larger increases in pH_i, at constant pH_o, cause no sustained change in vessel diameter. We produced these pH_i increases either by applying a weak base (i.e. NH_3 or TMA) or withdrawing a weak acid (i.e. acetic acid or CO_2). If increases in pH_i played an important role in alkalinization-induced cerebral vasoconstriction, then one would expect that applying a weak base or withdrawing a weak acid would be more effective at vasoconstriction than would be extracellular alkalinization.

It might be argued that the lack of vasoconstriction in the presence of a weak base is a toxic effect of the base on muscle contraction. However, we also observed no vasoconstriction when we elevated pH_i by withdrawing acetic acid or CO_2. In this latter case, the increase in pH_i occurred at a time when the cell was essentially free of the acid. In several of these experiments, we increased pH_o from 7·3 to 7·8 after the acetate or CO_2 washout, always observing a robust vasoconstriction. Thus, a long-lasting toxic inhibition of smooth muscle contraction by acetate and CO_2 is unlikely.

Our findings extend the work of others on the mechanism of alkalinization-induced cerebral vasoconstriction in two important ways. First, although others have suggested that this vasoconstriction is due to an increase in pH_o (Kontos *et al.* 1977*a*, *b*; Dacey & Duling, 1982), their conclusions rested on the assumption that respiratory alkalosis causes a greater increase in pH_i than does metabolic alkalosis. Our work confirms this assumption. Second, we have excluded a direct vasoconstricting effect of increased pH_i.

Comparison with work on other systemic arterial vessels

Work on rat aortic rings has shown that an exposure to NH_3–NH_4^+ at constant pH_o causes contraction (Danthuluri & Deth, 1989). In parallel experiments on cultured vascular smooth muscle cells, these authors showed that the NH_3–NH_4^+ caused pH_i to increase to a maximal value within 1 min. However, because the constriction of the rings developed with a latency of at least 4 min, it is unlikely that the contraction is caused exclusively by an increase in pH_i.

Constrictions caused by intracellular alkalinization have also been reported in rat mesenteric arterioles. Austin & Wray (1993) exposed strips of rat mesenteric artery to alkaline solutions while simultaneously monitoring muscle tension and pH_i. These investigators observed that an increase in pH_o caused an increase in tension that was accompanied by a large and rapid increase in pH_i, which reflected more than 70% of the change in pH_o. Because constriction elicited by increased pH_o was reversed by the simultaneous application of butyric acid, which reversed the increase in pH_i (at constant, elevated pH_o), the authors concluded that pH_o increases cause vasoconstriction in mesenteric arterioles only indirectly, after being transduced into pH_i increases. This conclusion was supported by the observation that application of the weak base trimethylamine at constant pH_o caused both an increase in pH_i and vasoconstriction. In contrast to contractions of rat aortic rings (Danthuluri & Deth, 1989), no latency in alkalinization-induced contraction of mesenteric artery strips was observed (Austin & Wray, 1993): contractions were maximal within 1–2 min. The time course of increases in mesenteric arteriolar tension was indeed quite similar to the time course of cerebral arteriolar constriction reported here. It is unclear why rat cerebral arterioles in the present study differ so remarkably from mesenteric vascular smooth muscle, both in the magnitude of the increase in pH_i with extracellular alkalinization and in the vasomotor response to intracellular alkalinization. Possible explanations of the differences between our results and those of Austin & Wray include physiological differences between cerebral and mesenteric vessels; methodological differences in the techniques used to alter or measure pH_i and vascular tone; the generation of vessels studied; and the amount of preload applied to the vessels.

Buffering system

We found that vasoconstriction upon extracellular alkalinization occurs in both Hepes-buffered and CO_2–HCO_3^--buffered solutions. Moreover, intracellular alkalinization alone is ineffective at causing vasoconstriction in either Hepes-buffered or CO_2–HCO_3^--buffered solutions. Thus, vasoconstriction is readily produced by hypocapnic (i.e. respiratory) alkalosis in HCO_3^--buffered solutions, but no constriction is observed during extracellular isohydric hypocapnia despite nearly equivalent increases in pH_i.

Acidification-induced constriction

Another interesting finding in the experiments presented here is that vessel constriction was frequently observed at the times that pH_i was decreased. Transient constrictions were often observed upon NH_4^+ and TMA washout and upon the initial exposure to acetate and CO_2. This constriction upon NH_4^+ washout has also been reported as an incidental finding by others in vascular tissue of non-cerebral origin (Furtado, 1987; Aalkjaer & Cragoe, 1988;

Danthuluri & Deth, 1989). The observation of constriction coincident with intracellular acidosis caused by four independent methods suggests that constriction does not reflect a toxic effect of the NH_4^+ but rather represents a direct effect of low pH_i on vessel tone. This might arise from regulatory effects of pH_i on excitation–contraction coupling or as a consequence of pH_i regulatory processes serving to restore pH_i to its resting value.

Possible mechanisms of vasoconstriction induced by increased pH_o

Several mechanisms have been proposed that are consistent with our data and account for alkalinization-induced cerebral vasoconstriction. One possible mechanism is cell depolarization, which could occur as a consequence of altered ion channel function, and which would result in an increase in the force of contraction. pH-dependent modulation of macroscopic and single-channel ion currents has been demonstrated for a number of ion channel types. Indeed, Harder (1982) and Harder & Madden (1985) have demonstrated that extracellular alkalinization leads to a depolarization of cerebral vascular smooth muscle cells, apparently mediated by a decrease in outward K^+ current. Others have reported that alkalinization causes increases in inward Ca^{2+} currents, which would similarly depolarize the smooth muscle cell (West, Leppla & Simard, 1992). It is also conceivable that H^+ itself carries current across the cell membrane (DeCoursey, 1991; Demaurex, Grinstein, Jaconi, Schlegal, Lew & Krause, 1992). If this were true in cerebral vascular smooth muscle cells, then the transmembrane H^+ gradient would directly affect membrane potential, and contraction might depend on the difference between pH_o and pH_i. However, the H^+ equilibrium potential is expected to become progressively more negative as pH_o increases. This would result in less inward H^+ current with extracellular alkalinization, and hyper- rather than depolarization. Thus, it is unlikely that changes in H^+ currents underlie alkalinization-induced constrictions.

A second general group of mechanisms proposed to account for alkalinization-induced constriction includes a number of paracrine second messengers that respond to acid–base disturbances. These include endothelial-derived relaxing factor (nitric oxide) (Iadecola, 1992; Wang, Paulson & Lassen, 1992; Pelligrino, Koenig & Albrecht, 1993) and prostaglandins (Wagerle & Mishra, 1988). Evidence that these second messengers participate in the response to acid–base disturbances derives from the findings that inhibitors of nitric oxide synthase and prostaglandin synthesis inhibit the vasodilation elicited by extracellular acidification. However, a role for these mediators in the response to alkalinization has yet to be reported.

Aalkjaer, C. & Cragoe, E. J. (1988). Intracellular pH regulation in resting and contracting segments of rat mesenteric resistance vessels. *Journal of Physiology* **402**, 391–410.

Apkon, M. & Boron, W. F. (1993). Na–H exchange in vascular smooth muscle of perfused cerebral arterioles: enhancement by prior acidification. *Pediatric Research* **33**, 30A.

Apkon, M. & Boron, W. F. (1994*a*). Extracellular alkalinization and intracellular acidification constrict penetrating cerebral arterioles. *FASEB Journal* **8**, A1032.

Apkon, M. & Boron, W. F. (1994*b*). Differential effects of intra- (pH_i) and extra- (pH_o) cellular pH on cerebral arteriolar tone. *Pediatric Research* **35**, 48A.

Austin, C. & Wray, S. (1993). Extracellular pH signals affect rat vascular tone by rapid transduction into intracellular pH changes. *Journal of Physiology* **466**, 1–8.

Binstock, L. & Lecar, H. (1969). Ammonium ion currents in the squid giant axons. *Journal of General Physiology* **53**, 342–361.

Boron, W. F. & De Weer, P. (1976). Intracellular pH transients in squid giant axons caused by CO_2, NH_3 and metabolic inhibitors. *Journal of General Physiology* **67**, 91–112.

Boyarsky, G., Ganz, M. B., Sterzel, B. & Boron, W. F. (1988). pH regulation in single glomerular mesangial cells. I. Acid extrusion in absence and presence of HCO_3. *American Journal of Physiology* **255**, C844–856.

Buckler, K. J., Vaughan-Jones, R. D., Peers, C., Lagadic-Gossman, D. & Nye, P. C. G. (1991). Effects of extracellular pH, P_{CO_2} and HCO_3^- on intracellular pH in isolated type-1 cells of the neonatal rat carotid body. *Journal of Physiology* **444**, 703–721.

Burg, M., Grantham, J., Abramow, M. & Orloff, J. (1966). Preparation and study of fragments of single rabbit nephrons. *American Journal of Physiology* **210**, 1293–1298.

Dacey, R. G. Jr & Duling, B. R. (1982). A study of rat intracerebral arterioles: methods, morphology, and reactivity. *American Journal of Physiology* **12**, H598–606.

Dacey, R. G. Jr & Duling, B. R. (1984). Effect of norepinephrine on penetrating arterioles of rat cerebral cortex. *American Journal of Physiology* **246**, H380–385.

Danthuluri, N. R. & Deth, R. C. (1989). Effects of intracellular alkalinization on resting and agonist-induced vascular tone. *American Journal of Physiology* **256**, H867–875.

DeCoursey, T. E. (1991). Hydrogen ion currents in rat alveolar epithelial cells. *Biophysical Journal* **60**, 1243–1253.

Demaurex, N., Grinstein, S., Jaconi, M., Schlegel, W., Lew, D. P. & Krause, K. H. (1992). Proton currents in human granulocytes: regulation by membrane potential and intracellular pH. *Journal of Physiology* **466**, 329–344.

Duling, B. R., Gore, R. W., Dacey, R. G. & Damon, D. N. (1981). Methods for isolation, cannulation, and *in vitro* study of single microvessels. *American Journal of Physiology* **241**, H108–116.

Ellis, D. & Thomas, R. C. (1976). Direct measurement of the intracellular pH of mammalian cardiac muscle. *Journal of Physiology* **262**, 755–771.

Furtado, M. (1987). Effect of NH_4Cl on the contractility of isolated vascular smooth muscle. *Life Sciences* **41**, 95–102.

Harder, D. R. (1982). Effect of H^+ and elevated P_{CO_2} on membrane electrical properties of rat cerebral arteries. *Pflügers Archiv* **394**, 182–185.

Harder, D. R. & Madden, J. A. (1985). Cellular mechanism of force development in cat middle cerebral artery by reduced P_{CO_2}. *Pflügers Archiv* **403**, 402–404.

HILLE, B. (1973). Potassium channels in myelinated nerve. *Journal of General Physiology* **61**, 669–686.

IADECOLA, C. (1992). Does nitric oxide mediate the increases in cerebral blood flow elicited by hypercapnia. *Proceedings of the National Academy of Sciences of the USA* **89**, 3913–3916.

KONTOS, H. A., RAPER, A. J. & PATTERSON, J. L. JR (1977*a*). Analysis of vasoactivity of local pH, P_{CO_2} and bicarbonate on pial vessels. *Stroke* **8**, 358–360.

KONTOS, H. A., WEI, E. P., RAPER, A. J. & PATTERSON, J. L. JR (1977*b*). Local mechanism of CO_2 action on cat pial arterioles. *Stroke* **8**, 226–229.

PEASE, D. C. (1962). Arterial and arteriolar systems. Microscopic and submicroscopic anatomy. In *Blood Vessels and Lymphatics*, chap. 1, ed. ABRAMSON, D. I., pp. 12–25. Academic Press, New York.

PELLIGRINO, D. A., KOENIG, H. M. & ALBRECHT, R. F. (1993). Nitric oxide synthesis and regional cerebral blood flow responses to hypercapnia and hypoxia in the rat. *Journal of Cerebral Blood Flow and Metabolism* **13**, 80–87.

RHODIN, J. A. G. (1980). Architecture of the vessel wall. In *Handbook of Physiology*, section 2, *The Cardiovascular System*, vol. II, *Vascular Smooth Muscle*, ed. BOHR, D. F., SOMLYO, A. P. & SPARKS, H. V. JR. American Physiological Society, Bethesda, MD, USA.

ROY, C. S. & SHERRINGTON, C. S. (1890). The regulation of the blood supply of the brain. *Journal of Physiology* **11**, 85–108.

THOMAS, J. A., BUCHSBAUM, R. N., ZIMNIAK, A. & RACKER, E. (1979). Intracellular pH measurements in Ehrlich ascites tumor cells utilizing spectroscopic probes generated in situ. *Biochemistry* **81**, 2210–2218.

TOLKOVSKY, A. M. & RICHARDS, C. D. (1987). Na^+/H^+ exchange is the major mechanism of pH regulation in cultured sympathetic neurons: measurements in single cell bodies and neurites using a fluorescent pH indicator. *Neuroscience* **22**, 1093–1102.

WAGERLE, L. C. & MISHRA, O. P. (1988). Mechanism of CO_2 response in cerebral arteries of the newborn pig: Role of phospholipase, cyclooxygenase, and lipoxygenase pathways. *Circulation Research* **62**, 1019–1026.

WANG, Q., PAULSON, O. B. & LASSEN, N. A. (1992). Effect of nitric oxide blockade by N^G-nitro-L-arginine on cerebral blood flow response to changes in carbon dioxide tension. *Journal of Cerebral Blood Flow and Metabolism* **12**, 947–953.

WEST, G. A., LEPPLA, D. C. & SIMARD, J. M. (1992). Effects of external pH on ionic currents in smooth muscle cells from the basilar artery of the guinea pig. *Circulation Research* **71**, 201–209.

WILDING, T. J., CHENG, B. & ROOS, A. (1992). pH regulation in adult rat carotid body glomus cells. Importance of extracellular pH, sodium, and potassium. *Journal of General Physiology* **100**, 593–608.

WRAY, S. (1988). Smooth muscle intracellular pH: measurement, regulation, and function. *American Journal of Physiology* **254**, C213–225.

Acknowledgements

We gratefully acknowledge the assistance of John Geibel, MD, DSc, who assisted us with the confocal microscopy. This work was supported by a Physician Postdoctoral Fellowship Award by the Howard Hughes Medical Institute (M. A.)

Received 30 July 1994; accepted 11 October 1994.